

Effect of post annealing on structural and optical properties of ZnO thin films deposited by vacuum coating technique

C. Periasamy · Rajiv Prakash · P. Chakrabarti

Received: 6 December 2008 / Accepted: 5 May 2009
© Springer Science+Business Media, LLC 2009

Abstract We report the effect of annealing temperature on structural, electrical and optical properties of polycrystalline zinc oxide thin films grown on p-type silicon (100) and glass substrates by vacuum coating technique. The XRD and AFM measurements confirmed that the thin films grown by this technique have good crystalline hexagonal wurtzite structures and homogenous surfaces. The study also reveals that the rms value of thin film roughness increases from 6 to 16 nm, the optical band gap increases from 3.05 to 3.26 eV and resistivity from 0.3 to 5 Ωcm when the post-deposition annealing temperature is changed from 400 to 600 °C. It is observed that ZnO thin film annealed at 600 °C after deposition provide a smooth and flat texture suited for optoelectronic applications.

1 Introduction

The synthesis and characterization of ZnO thin film have drawn considerable attention of the researchers in view of the excellent electrical and optical properties of the

materials [1–3]. The multifunctional material has emerged as a material of choice in a number of novel optoelectronic devices including thin film transistor (TFT) and solar cells [4–8]. Zinc oxide (ZnO) has a direct band gap of 3.37 eV and a high value exciton binding energy (60 meV) [1]. The nanostructure grain size of ZnO film can be exploited for improving the performance of various optoelectronics devices. Different methods of growing zinc oxide thin film with consistent morphology and reproducible optical and electrical properties with long-term stability have been tried in the past by the researchers. These techniques for growing ZnO films on a variety of substrates include pulsed laser deposition (PLD) [9], sol–gel technique [10, 11], reactive evaporation [12], chemical vapor deposition (CVD) [13–15], metal organic chemical vapor deposition (MOCVD) [16, 17], RF sputtering [18] and thermal evaporation technique [19]. Among the above techniques, the vacuum evaporation-deposition technique has several distinct advantages, e.g. process simplicity, cost effectiveness and easy thickness monitoring over a very large area. However, the important crystalline properties of ZnO thin films strongly depend on the growth condition, growth techniques and the substrate. The grain growth of the ZnO thin film on a silicon substrate is generally high. The advantages of silicon substrate are its low cost, easy availability and sensitivity to thermal effects and integrated circuit capability.

In the present paper we report deposition of ZnO thin film on p-type silicon with (100) orientation and silica glass substrates by vacuum coating technique at room temperature. The thin films were subsequently annealed in two different batches at 400 and 600 °C. The samples were further investigated for their structural, electrical and optical properties.

C. Periasamy · P. Chakrabarti (✉)
Centre for Research in Microelectronics,
Department of Electronics Engineering,
Institute of Technology, Banaras Hindu University,
Varanasi 221-005, India
e-mail: pchakrabarti.ece@itbhu.ac.in

R. Prakash
School of Materials Science and Technology,
Institute of Technology, Banaras Hindu University,
Varanasi 221-005, India

2 Experimental

2.1 ZnO thin film preparation

Zinc oxide (ZnO) thin films were deposited on p-type Silicon (100) substrate and glass substrate in separate batches by vacuum coating technique using a high-purity ZnO 99.99% (15 g 4N) powder supplied by MERK-Chemical limited Mumbai, India as source materials. The vacuum coating setup unit (Model no 12A4D of HIND-VAC, India make) is used for the deposition purpose. Before deposition the substrates were cleaned using trichloroethylene methanol and acetone sequentially. The dried substrate was rubbed gently with cotton. The details of deposited parameters of ZnO thin film are listed in Table 1. The distance between substrate to source was fixed 18 cm apart. The vacuum coating chamber was evacuated to 3×10^{-5} mPa using a diffusion pump. The substrate was pre-evaporated before deposition for 10 min in order to remove any dust particles on the substrate surface. The heating filament was a conventional molybdenum boat. The in-built digital crystal thickness monitor was used for monitoring the film thickness. A home variac type discharge source was maintained at a potential from 100 to 130 V with discharge current of 3–6 A. The pressure was brought down until a vacuum of about 3×10^{-3} mbar was achieved. The film was subjected to rapid thermal annealing after deposition at selected temperatures (400 and 600 °C) in nitrogen (N₂) environment (with a purity of 99.99%) for 20 min in order to improve the quality of ZnO thin film crystal and its conductivity. The film was then left to cool down to room temperature before carrying out the electrical and optical measurements. The sheet conductivity of Silicon (100) substrate was measured by four-probe method before deposition. The sheet resistivity was found to be in the range of 4–8 Ωcm.

Table 1 Deposition details of ZnO thin film by vacuum coating technique

Deposition parameter	Conditions
Substrates	p-type silicon (100) and glass substrates
Source material	ZnO 99.99% (15 g) powder
Base pressure	3×10^{-3} mbar
Substrate cleaned by	Using trichloroethylene methanol and acetone sequentially
The distance between substrate to source	18 cm apart
ZnO film thickness	300 nm
Deposition time	50 min

2.2 Sample characterization

Zinc oxide (ZnO) thin film samples grown on silicon substrates were examined by X-ray diffraction (XRD) using 18-Kw rotating anode Rigku powder diffractometer with slow scanning speed $2\theta/\text{min}$ and parabolic filter CuK α radiation. The X-ray results show that the deposited ZnO samples are in the polycrystalline state. Optical measurements were carried out by UV–V is spectrophotometer (Perkin Elmer, Germany made, and Model No. Lamda-25). Atomic force microscope (AFM; NT-MDT; Russia made, Model No. SOL-PRO 47) measurements in semi-conduct mode and 1 Hz scan rate were made on the ZnO thin films in order to investigate the surface morphology, roughness, grain size etc.

3 Results and discussions

3.1 Structural studies

Figure 1a and b show the intensity versus 2θ XRD pattern of nanocrystalline ZnO films deposited by vacuum coating technique on p-type Si (100) substrate for samples annealed at 400 and 600 °C, respectively. This result clearly shows that ZnO thin film deposited by this method is polycrystalline in nature. Further, the quality of ZnO thin film and its crystallinity are better for the sample annealed at 600 °C. The XRD pattern of deposited ZnO thin films shows typically one peak at $2\theta = 34.12$ (002) and another peaks at $2\theta = 61.90$ (103). These peaks confirmed that ZnO thin films grown on Silicon (100) substrate are C-axis oriented. The extracted crystallite size from XRD spectrum of thin film is 30 ± 10 nm. The crystallite size was estimated by the Debye–Scherrer relation

$$d = \frac{c \lambda}{\beta \cos \theta} \quad (1)$$

where β is the full width at half maximum of X-ray peak, d is the crystallite size, λ is the X-ray wavelength and c is the correction factor taken as 0.90 in the calculation.

3.2 Surface morphology study by AFM

The surface morphology of deposited ZnO thin film on Silicon (100) and glass substrates were studied by atomic force microscope (AFM) (Sol-Pro 47 Russian made). The 2D and 3D AFM images were scanned in semi-conduct mode with a gold-coated SiN tip. The AFM scanning details are listed in Table 2.

The grain particle size was calculated using AFM analysis software. The average value of ZnO grain particle size ranges between 20–45 nm for samples grown on Si

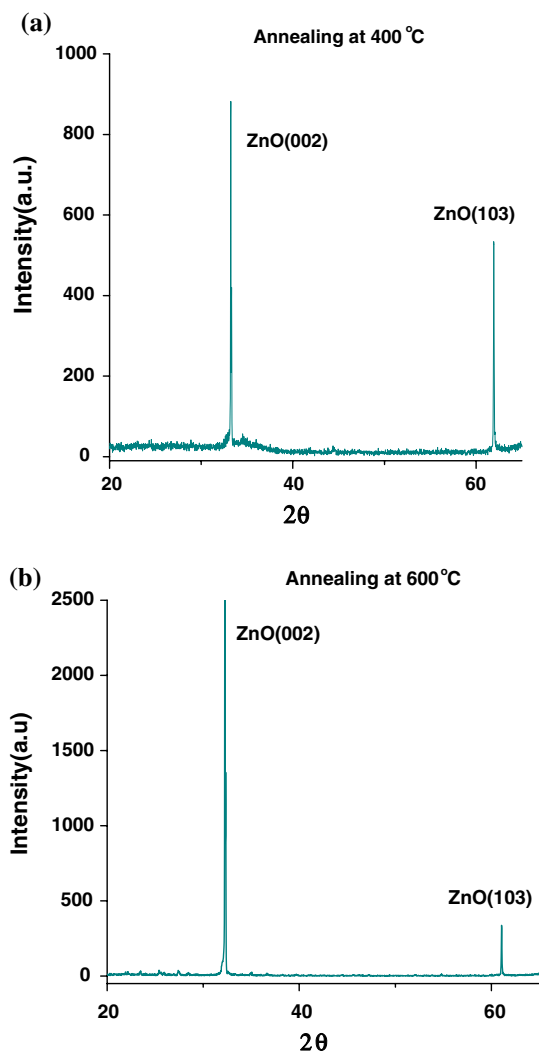


Fig. 1 X-ray Diffraction (XRD) patterns of the ZnO film deposited onto the silicon substrate, film post annealed: (a) 400 °C, (b) 600 °C

Table 2 AFM scanning details

AFM model no	Sol-Pro 47
Scanning mode	Semi conduct mode (topography)
Scanning speed	1 Hz, 256 pixels per line
Resonant frequency	256 KHz
Scanning tip material	SiN, thickness (1.7 μm)
Spring constant	8 N/m

and 30–50 nm for samples grown on glass and both annealed at 400 °C. The Fig. 2a–b and 2c–d illustrate the 2D and 3D scanning AFM images of the samples annealed at 400 °C for ZnO films grown on Silicon (100) and glass substrates, respectively. The Fig. 3a–b and 3c–d illustrate the corresponding 2D and 3D AFM images of ZnO thin film samples annealed at 600 °C. By comparing and contrasting the 2D and 3D images shown in Figs. 2 and 3 it is

found that silicon (100) substrate gives a better quality ZnO film as compared to glass substrate and the grain size increases at higher annealing temperature in each case. The AFM images further reveal that a good quality homogeneous film across entire surface can be grown by vacuum coating technique. It is further seen that an increase in annealing temperature results in the conversion of pyramidal surface morphology with columnar grains to relatively flat surface with increasing grain size. The effect of annealing temperature on the characteristics of the film such as grain size and roughness of the surface morphology are summarized in Table 3.

The surface roughness of the ZnO thin film was calculated in terms of root mean square (rms) value by using AFM software. The rms value of ZnO thin film roughness is estimated to be 6 and 16 nm for annealing temperature 400 and 600 °C, respectively. Figure 4 depicts the variation of surface roughness of ZnO film with annealing temperature. It is seen that both average growth size and surface roughness increase with increasing annealing temperature. The rms value of roughness can be estimated using the formula

$$R(\text{rms}) = \left(\frac{\sum_{i=1}^N (Z_i - Z_{\text{ave}})^2}{N} \right)^{1/2} \tag{2}$$

where Z_i is the value of Z at i th pointing, Z_{ave} is the average of the Z value and N is number of points.

3.3 Absorbance study

The optical characterization of ZnO samples was carried out by using double beam spectrophotometer in the wavelength range from 200–1,000 nm. The absorbance of substrate was corrected by placing an uncoated glass of the same size as the reference. Figure 5 shows the variation of absorbance of ZnO film grown on glass substrate with wavelength. It is seen from the figure that the maximum absorption occurs at 390 nm and remains significant over the entire UV range and decay exponentially in the longer wavelength for sample annealed at 400 °C. It is further seen that the peak absorbance drops drastically for the sample annealed at 600 °C but the absorbance maintains a relatively high value in the entire UV–Visible region as compared to the sample annealed at 400 °C. The absorption coefficient (α) has been calculated using Eq. (3) given by

$$\alpha = \frac{1}{t} \left(\ln \left(\frac{1 - R(\lambda)}{T(\lambda)} \right) \right) \tag{3}$$

where $R(\lambda)$ is the spectral reflectance at the measuring wavelength, $T(\lambda)$ is the spectral transmittance at the wavelength and t is the thickness of the film.

Fig. 2 a–d Top view and side view AFM image of the ZnO film grown on Silicon (100) and glass substrates: post annealed at 400 °C

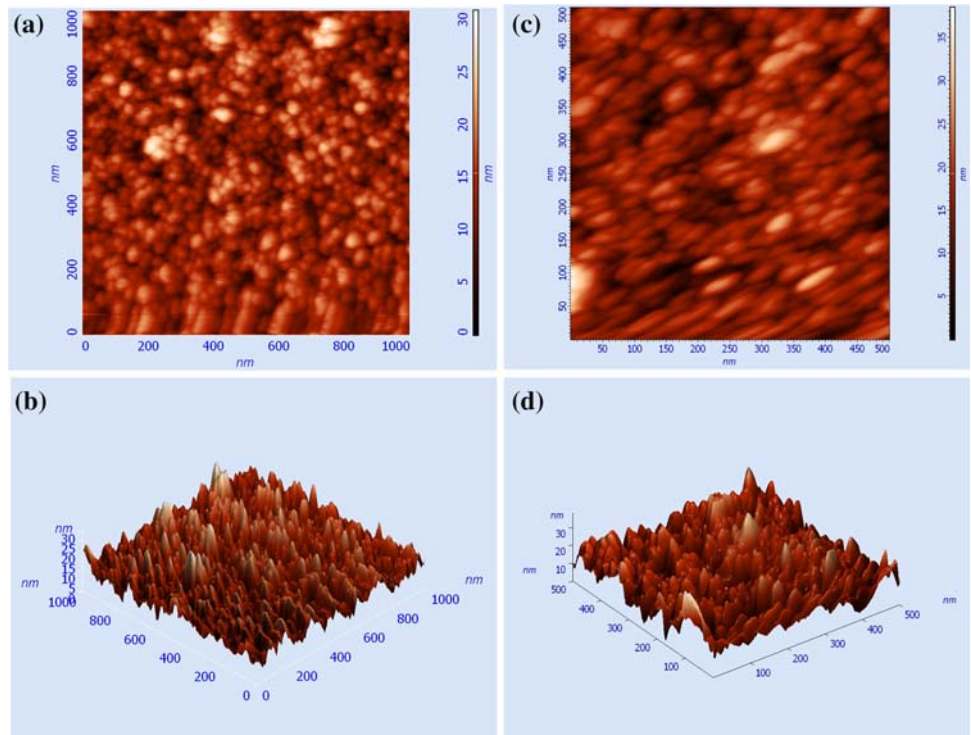
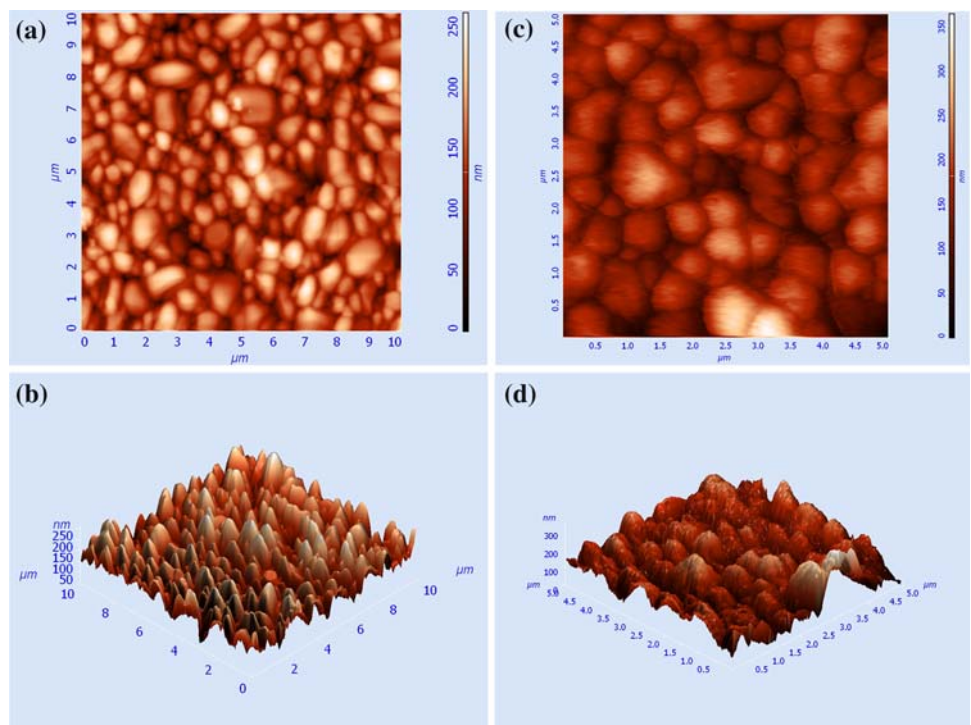


Fig. 3 a–d Top view and side view AFM image of the ZnO film grown on Si (100) and glass substrate: post annealed at 600 °C



The optical band gaps of ZnO samples were extracted from the absorbance spectra of ZnO thin film deposited on glass substrate. The band gap of ZnO thin film was estimated using standard equation given by

$$\alpha h\nu = A(h\nu - E_g)^{1/2} \tag{4}$$

where α is the absorption coefficient, $h\nu$ is the energy of absorbance light and A is a constant. Figure 6 shows the plot of $(\alpha h\nu)^2$ versus the photon energy ($h\nu$) for the two samples of ZnO/Glass substrate films annealed at 400 and 600 °C. The energy gap can be estimated from the extrapolation of the linear portion of $(\alpha h\nu)^2$ vs. $h\nu$ plot to

Table 3 The effect of annealing temperature resulted on surface morphology of ZnO thin film and its corresponding AFM result

Substrate type	Deposited thin film	Annealing temperature in °C	Grain size in nm	Roughness in nm	Crystalline type
Si	ZnO	400	30	16	Polycrystalline
Glass	ZnO	400	40	21	Polycrystalline
Si	ZnO	600	800	6	Polycrystalline
Glass	ZnO	600	900	13	Polycrystalline

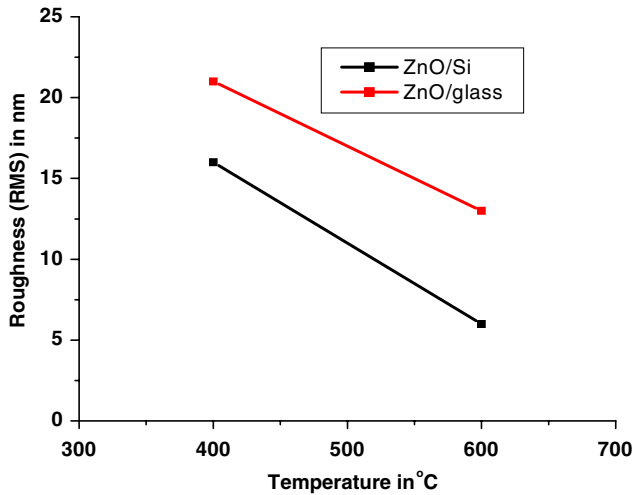


Fig. 4 Plot of ZnO roughness (rms) versus post annealing temperature

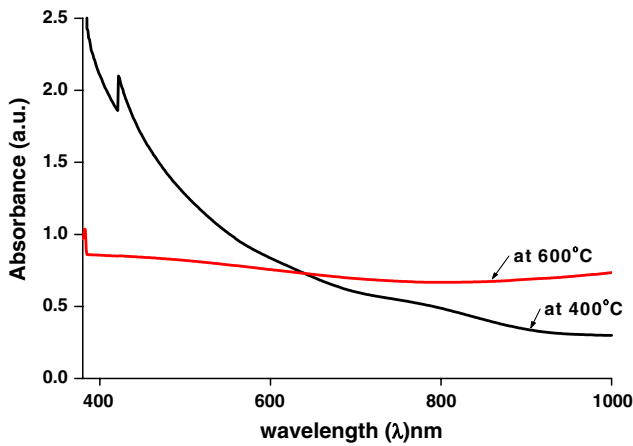


Fig. 5 Plot of absorbance versus wavelength for the ZnO thin film samples annealed at 400 and 600 °C

cut the energy axis at $\alpha = 0$. The values of energy band gap were estimated to be 3.05 and 3.26 eV for the ZnO samples annealed at 400 and 600 °C, respectively. It is seen that the band gap of the ZnO film estimated from the absorbance study improves with annealing temperature and approach the value of 3.3 eV reported for bulk ZnO [20]. This may be accounted for the fact that the quality of the ZnO film improves when the sample is annealed at a higher

temperature (in this case 600 °C). This fact is also by the AFM images shown in Figs. 2a–d and 3a–d.

3.4 Resistivity study

The conduction characteristics of ZnO thin films are determined by the electrons generated from O^{2-} vacancies and Zn interstitial atoms. The electrical characterization of ZnO samples (annealed at 600 and 400 °C) were carried out using four probe measurements for samples grown on Silicon (100) and glass substrates at room temperature conditions. The resistivity was calculated from sheet resistivity of thin film layer by using the following relationship

$$\rho = \frac{\pi}{\ln 2} \left(\frac{V}{I} \right) \times t \tag{5}$$

where V is the voltage measured across the inner probes, I is the current applied through outer probes and t is the thickness of thin film. It was observed that the sheet resistivity of ZnO thin film layer decreases from 5 Ωcm for samples annealed at 400 °C to 0.3 Ωcm for samples annealed at 600 °C. The resistivity of ZnO thin film is related to the carrier mobility by the standard relation

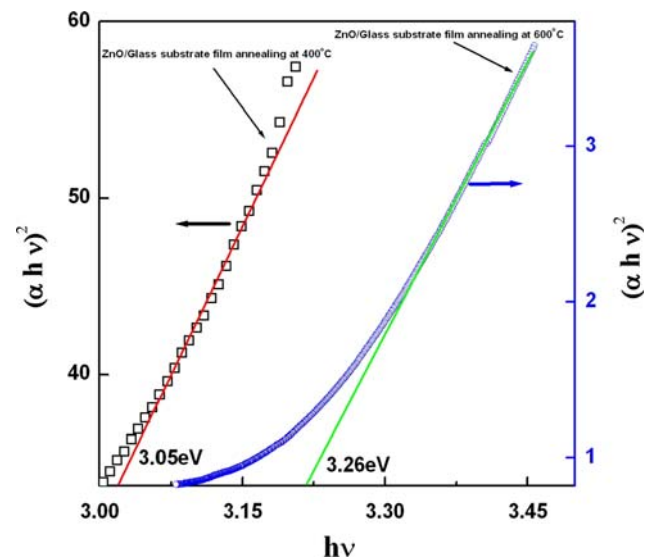


Fig. 6 Plot of $(\alpha hv)^2$ versus Photon energy (eV) for the ZnO/Galss substrate thin film samples annealed at 400 and 600 °C

$$\rho = \frac{1}{nq\mu} \quad (6)$$

where q is the electron charge and μ is the carrier mobility and n is the concentration.

The XRD and AFM images confirm that the ZnO samples grown on both the substrates are of polycrystalline form. In polycrystalline materials (in the present case of ZnO films) the crystallinity and microstructure are essentially determined by grain size. The grain size variation in turn is responsible for a change in the mobility value of the carriers in the film. The grain size is found to increase from 30 nm for samples annealed at 400 °C to 800 nm for samples annealed at 600 °C in the case of films grown on Silicon (100) substrate. Therefore, the grain boundary density and carrier diffusion decrease in the later case. The increased grain size results in an increase in mobility. Figure 7 shows that the resistivity decreases when the post deposition annealing temperature is increased. The AFM images depicted in Fig. 8a–b illustrate the long-term stability of the samples annealed at 600 °C. The study of AFM surface morphology of samples scanned 10 weeks after the date of deposition (Fig. 8b) exhibited the same properties in terms of surface morphology, grain size and roughness as did the samples on the date of deposition. This demonstrates that our ZnO thin films deposited by vacuum coating technique have consistent morphology and long-term stability. The reproducibility is also checked by studying samples prepared in different batches.

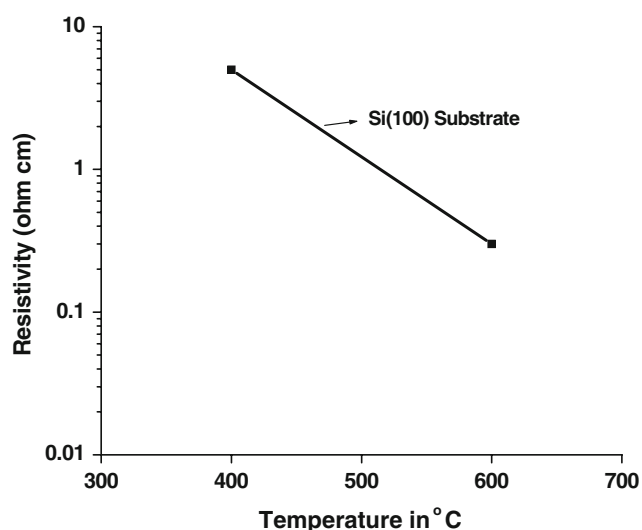


Fig. 7 Plot of resistivity versus temperature

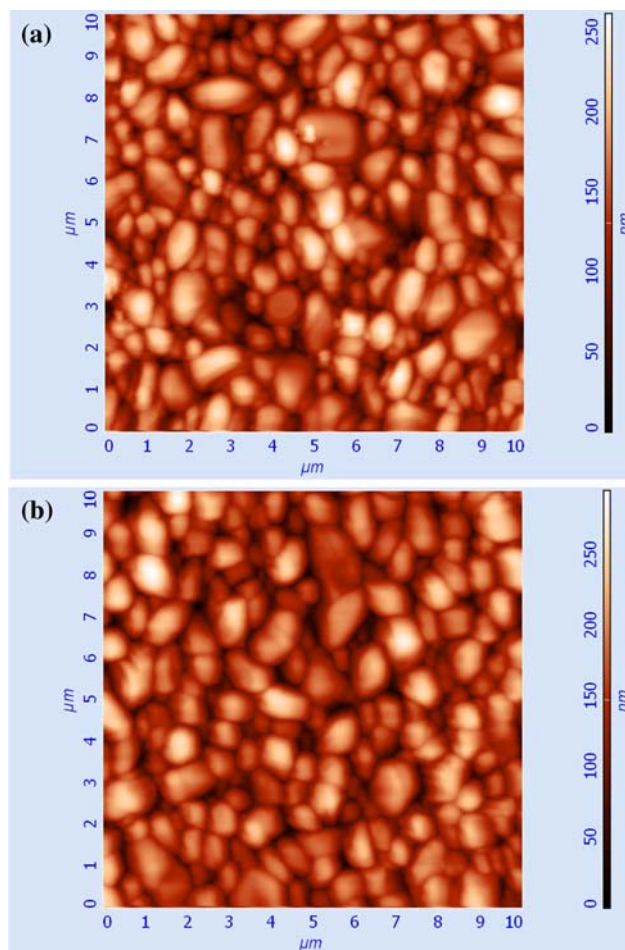


Fig. 8 Illustrating ZnO thin films stability: The AFM scanning image of film (a) on date of deposition, (b) after 10 weeks from the date of deposition

4 Conclusions

Zinc oxide (ZnO)/Si thin films were deposited by vacuum coating technique. The effect of annealing temperature on the microstructure, electrical and optical properties of ZnO thin films were studied by XRD, AFM, four probe and UV–Visible measurements. The XRD results reveal that the deposited thin film has a good polycrystalline hexagonal wurtzite structure. The AFM results demonstrate that a uniform surface morphology over the entire surface can be obtained by this technique. The technique can be used to develop stable and reproducible thin film with excellent surface morphology by post deposition annealing at high temperature (600 °C). The quality of the post-deposition annealed ZnO films grown by vacuum evaporation-deposition technique is comparable with that grown by other techniques. The minimum roughness value is as low as 6 nm. The increase in annealing temperature results into a relatively flat surface with increased grain size which results in increased mobility. This feature would be

especially attractive for fabrication of thin film transistor (TFT). The study also revealed that Silicon (100) is a better substrate as compared to glass for thin film deposition of ZnO by vacuum coating technique.

Acknowledgments The authors wish to thank Prof. D. Pandey, School of Materials Science and Technology, Institute of Technology, Banaras Hindu University, Varanasi, India, for helpful discussions.

References

1. S.Y. Hu, Y.C. Lee, J.W. Lee, J.C. Huang, J.L. Shen, W. Water. *Appl. Surf. Sci.* **254**, 1578 (2008). doi:[10.1016/j.apsusc.2007.07.134](https://doi.org/10.1016/j.apsusc.2007.07.134)
2. L. Zhang, H. Zhang, Y. Bai, J.W. Ma, J. Cao, X.Y. Jiang, Z.L. Zhang, *Solid. State. Commun.* **146**, 387 (2008). doi:[10.1016/j.ssc.2008.03.036](https://doi.org/10.1016/j.ssc.2008.03.036)
3. M. Bouderbala, S. Hamzaoui, B. Amrani, H. Ali, M. Reshak, M. Adnane, T. Sahraoui, M. Zerdali, *Physica. B* **403**, 3326 (2008). doi:[10.1016/j.physb.2008.04.045](https://doi.org/10.1016/j.physb.2008.04.045)
4. B.J. Norris, J. Anderson, J.F. Wager, D.A. Keszler, *J. Phys., D. Appl. Phys. (Berl)* **36**, L105 (2003)
5. R.L. Hoffman, B.J. Norris, J.F. Wager, *Appl. Phys. Lett.* **82**, 733 (2003). doi:[10.1063/1.1542677](https://doi.org/10.1063/1.1542677)
6. H.S. Bae, S. Im, *J. Vac. Sci. Technol. B* **22**(3), 1191 (2004). doi:[10.1116/1.1756166](https://doi.org/10.1116/1.1756166)
7. K. Remashan, J.H. Jang, D.K. Hwang, S.J. Park, *Appl. Phys. Lett.* **91**, 182101 (2007). doi:[10.1063/1.2804566](https://doi.org/10.1063/1.2804566)
8. E. Fortunato, P. Barquinha, A. Pimentel, A. Goncalves, A. Marques, L. Pereira, R. Martins, *Thin. Solid. Films.* **487**, 205 (2005). doi:[10.1016/j.tsf.2005.01.066](https://doi.org/10.1016/j.tsf.2005.01.066)
9. W.J.E. Beek, M.M. Wienk, R.A.J. Janssen, *J. Mater. Chem.* **15**, 2985 (2005). doi:[10.1039/b501979f](https://doi.org/10.1039/b501979f)
10. S. Mandal, M.L.N. Goswami, K. Das, A. Dhar, S.K. Ray, *Thin. Solid. Films.* **516**, 8702 (2005). doi:[10.1016/j.tsf.2008.05.016](https://doi.org/10.1016/j.tsf.2008.05.016)
11. G. Srinivasan, J. Kumar, *Cryst. Res. Technol.* **41**, 893 (2006). doi:[10.1002/crat.200510690](https://doi.org/10.1002/crat.200510690)
12. D. Yuvaraj, K. Narasimha Rao, *Vacuum* **82**, 1274 (2008). doi:[10.1016/j.vacuum.2008.03.043](https://doi.org/10.1016/j.vacuum.2008.03.043)
13. J.G. Lu, T. Kawaharamura, H. Nishinka, Y. Kamada, T. Ohshima, S. Fujita, *J. Cryst. Growth.* **299**, 1 (2007). doi:[10.1016/j.jcrysgro.2006.10.251](https://doi.org/10.1016/j.jcrysgro.2006.10.251)
14. V.R. Shinde, T.P. Gujar, C.D. Lokhande, *Sol. Energy Mater. Sol. Cells* **91**, 1055 (2007). doi:[10.1016/j.solmat.2007.02.017](https://doi.org/10.1016/j.solmat.2007.02.017)
15. M. Purica, E. Budianu, E. Rusu, M. Danila, R. Gavrilă, *Thin. Solid. Films.* **403–404**, 485 (2002). doi:[10.1016/S0040-6090\(01\)01544-9](https://doi.org/10.1016/S0040-6090(01)01544-9)
16. K.S. KIM, H.W. KIM, *J. Korean. Physical. Soc.* **42**, S149 (2003)
17. W.Z. Xu, Z.Z. Ye, Y.J. Zeng, L.P. Zhu, B.H. Zhao, L. Jiang, J.G. Lu, H.P. He, S.B. Zhang, *Appl. Phys. Lett.* **88**, 173506 (2006)
18. K. Prabakar, C. Kim, C. Lee, *Cryst. Res. Technol.* **40**, 1150 (2005). doi:[10.1002/crat.200410508](https://doi.org/10.1002/crat.200410508)
19. B.D. Yao, Y.F. Chan, N. Wang, *Appl. Phys. Lett.* **81**, 22 (2002). doi:[10.1063/1.1495878](https://doi.org/10.1063/1.1495878)
20. V. Srikant, D.R. Clarke, *J. Appl. Phys.* **83**, 5447 (1998). doi:[10.1063/1.367375](https://doi.org/10.1063/1.367375)